Nondiagonalizable and nondivergent susceptibility tensor in the Hamiltonian mean-field model with asymmetric momentum distributions

Yoshiyuki Y. Yamaguchi*

Department of Applied Mathematics and Physics, Graduate School of Informatics, Kyoto University, 606-8501 Kyoto, Japan

(Received 23 January 2015; revised manuscript received 30 June 2015; published 8 September 2015)

We investigate the response to an external magnetic field in the Hamiltonian mean-field model, which is a paradigmatic toy model of a ferromagnetic body and consists of plane rotators like *XY* spins. Due to long-range interactions, the external field drives the system to a long-lasting quasistationary state before reaching thermal equilibrium, and the susceptibility tensor obtained in the quasistationary state is predicted by a linear response theory based on the Vlasov equation. For spatially homogeneous stable states, whose momentum distributions are asymmetric with 0 means, the theory reveals that the susceptibility tensor for an asymptotically constant external field is neither symmetric nor diagonalizable, and the predicted states are not stationary accordingly. Moreover, the tensor has no divergence even at the stability threshold. These theoretical findings are confirmed by direct numerical simulations of the Vlasov equation for skew-normal distribution functions.

DOI: 10.1103/PhysRevE.92.032109 PACS number(s): 05.20.Dd, 05.70.Jk, 74.25.N−

I. INTRODUCTION

Long-range Hamiltonian systems have many remarkable features [1], and one of them is the existence of quasistationary states (QSSs) on the way to relaxation to thermal equilibrium. The lifetime of QSSs diverges with the number of particles constructing the system [2,3], and hence QSSs are solely observable in systems with a large population like self-gravitating systems [4]. The dynamics of such a system is described by the Vlasov equation, or the collisionless Boltzmann equation, in the limit of a large population [5–7], and the QSSs, including thermal equilibrium states, are regarded as stable stationary solutions to the Vlasov equation. The system slowly goes towards thermal equilibrium with a large but finite population due to finite-size effects [3,8].

The QSSs are observed not only in isolated systems, but also in systems under external fields. The initial QSS, which may or may not be in thermal equilibrium, is driven to another QSS by the external field, and the resulting QSS is not necessarily in thermal equilibrium. As a result, the response to the external field may differ from one obtained by statistical mechanics. Indeed, in the ferromagnetic so-called Hamiltonian mean-field (HMF) model [9,10], the critical exponents are obtained as $\gamma_- = 1/4$ [11] and $\delta = 3/2$ [12] with the aid of a linear [13,14] and a nonlinear [12] response theory based on the Vlasov description, respectively, while statistical mechanics gives $\gamma_- = 1$ and $\delta = 3$. Interestingly, with another exponent, $\beta = 1/2$, the nonclassical exponents satisfy the classical scaling relation $\gamma_- = \beta(\delta - 1)$ and have universality for initial reference families of QSSs in a wide class of one-dimensional mean-field models [15].

The universality is derived under the assumption that the initial distribution functions depend on position and momentum only through the one-particle Hamiltonian with reference to the Jeans theorem [16]. Thus, the initial states are symmetric with respect to momentum. The symmetric initial states are also used in studies on nonequilibrium statistical mechanics [17–20], the core-halo description of QSSs [21], nonequilibrium dynamics [22], and correlation and diffusion [23]. See also Refs. [1] and [24].

Nevertheless, asymmetric momentum distributions appear in beam-plasma systems (see [25–28] for instance) and are experimentally created in an ultracold plasma by optical pumping [29]. In the HMF model, homogeneous distributions are stationary even asymmetric, and it is, therefore, natural to seek the response in the asymmetric case to complete the response theory. The main purpose of this article is to investigate the linear response against asymptotically constant external field around spatially homogeneous but asymmetric distributions in the HMF model. It is worth noting that, despite its simpleness, the model shares similar dynamics with the free-electron laser [30] and an anisotropic Heisenberg model under classical spin dynamics [31].

The HMF model consists of plane rotators like *XY* spins, and the susceptibility tensor in the HMF model is of size 2×2, corresponding to the x and y directions of the rotators. For symmetric homogeneous states, the susceptibility tensor is directly diagonalized and experiences a divergence at the critical point of the second-order phase transition, which is dynamically interpreted as the stability threshold of the homogeneous states [13–15]. We then ask the two questions for asymmetric momentum distributions with 0 means: Is the susceptibility tensor symmetric and diagonalizable? Does the response diverge at the stability threshold? We answer these questions negatively. The nondiagonalizable response tensor implies that the external field for the x direction induces magnetization for the y direction, and such a response is unavoidable even when the coordinate is changed. Due to this nondiagonalizability, the predicted state is not stationary, while the constant external field may drive the system to a stationary state asymptotically. In other words, the nondiagonalizability provides an example of a discrepancy between the asymptotic states in the linear dynamics and the full Vlasov dynamics. The nondivergence of the response suggests that $\gamma_+ = 0$ and $\delta = 1$, and interestingly, the scaling relation $\gamma_+ = \beta(\delta - 1)$ holds, although β might not be well defined since spatially inhomogeneous stationary states must be symmetric by the Jeans theorem [16].

*yyama@amp.i.kyoto-u.ac.jp

This article is organized as follows. The HMF model and linear responses are reviewed in Sec. II. As an example of a family of asymmetric distributions, we introduce the skew-normal distributions and investigate their stability in Sec. III. Theoretical consequences are examined by direct numerical simulations of the Vlasov equation in Sec. IV. We discuss the stationarity of the predicted state in Sec. V. The last section, VI, is devoted to a discussion and summary.

II. THE HAMILTONIAN MEAN-FIELD MODEL AND LINEAR RESPONSE THEORY

A. The model

The HMF model with a time-dependent external magnetic field $\vec{h} = (h_x(t), h_y(t))$ is expressed by the Hamiltonian

$$H_N(q,p,t) = \sum_{j=1}^{N} \frac{p_j^2}{2} + \frac{1}{2N} \sum_{j,k=1}^{N} [1 - \cos(q_j - q_k)] - \sum_{j=1}^{N} [h_x(t) \cos q_j + h_y(t) \sin q_j]. \tag{1}$$

The corresponding one-particle Hamiltonian is defined on the μ space, which is $(-\pi,\pi] \times \mathbb{R}$, as

$$\mathcal{H}[f](q,p,t) = \frac{p^2}{2} - (M_x + h_x)\cos q - (M_y + h_y)\sin q, \tag{2}$$

where the magnetization vector (M_x, M_y) is defined by

$$(M_x, M_y) = \iint_{\mu} (\cos q, \sin q) f(q,p,t) \mathrm{d}q\mathrm{d}p. \tag{3}$$

The one-particle distribution function f is governed by the Vlasov equation

$$\frac{\partial f}{\partial t} + \{\mathcal{H}[f], f\} = 0, \tag{4}$$

with the Poisson bracket defined by

$$\{f,g\} = \frac{\partial f}{\partial p}\frac{\partial g}{\partial q} - \frac{\partial f}{\partial q}\frac{\partial g}{\partial p}. \tag{5}$$

One can straightforwardly check that any spatially homogeneous states, $f_0(p)$, are stationary if the external field $\vec{h}$ is absent.

We prepare a homogeneous stable stationary state $f_0(p)$ for $t < 0$ and add a small external field $\vec{h}$ for $t > 0$. To avoid an artificial rotation, we require a 0 mean for $f_0(p)$ and consider an asymptotically constant external field accordingly. For instance, we set

$$\begin{pmatrix} h_x(t) \\ h_y(t) \end{pmatrix} = \Theta(t) \begin{pmatrix} h_x \\ h_y \end{pmatrix} \tag{6}$$

using the Heaviside step function $\Theta(t)$, and the external field drives the initial state f_0 to $f = f_0 + f_1$ asymptotically. Accordingly, the one-particle Hamiltonian $\mathcal{H}[f]$ changes from H_0 to $H_0 + H_1$, where

$$H_0 = \frac{p^2}{2}, \quad H_1 = -(M_{1,x} + h_x)\cos q - (M_{1,y} + h_y)\sin q \tag{7}$$

and

$$M_{1,x} = \langle \cos q \rangle_1, \quad M_{1,y} = \langle \sin q \rangle_1. \tag{8}$$

We introduce the averages of an observable B with respect to f_0 and f_1 as

$$\langle B \rangle_j = \iint_{\mu} B(q,p) f_j(q,p) \mathrm{d}q\mathrm{d}p, \quad (j = 0,1). \tag{9}$$

B. Isothermal linear response

It might be instructive to review the isothermal linear response, to compare it with the Vlasov linear response theory, which is presented in the next subsection (Sec. II C). The thermal equilibrium states of the HMF model are described by the one-particle distribution functions of

$$f(q,p) = \frac{e^{-\beta(H_0+H_1)}}{\iint_{\mu} e^{-\beta(H_0+H_1)} \mathrm{d}q\mathrm{d}p}. \tag{10}$$

Hereafter β represents not one of the critical exponents mentioned in Sec. I, but the inverse temperature. Expanding f into the power series of H_1 and picking up to the linear order, we have

$$\langle B \rangle_1 = -\beta[\langle B H_1 \rangle_0 - \langle B \rangle_0 \langle H_1 \rangle_0]. \tag{11}$$

Substituting $\cos q$ and $\sin q$ into B, we have the matrix formula

$$\begin{pmatrix} M_{1,x} \\ M_{1,y} \end{pmatrix} = \begin{pmatrix} C_{xx} & C_{xy} \\ C_{yx} & C_{yy} \end{pmatrix} \left[\begin{pmatrix} M_{1,x} \\ M_{1,y} \end{pmatrix} + \begin{pmatrix} h_x \\ h_y \end{pmatrix} \right], \tag{12}$$

where the correlation matrix $\mathbf{C} = (C_{\nu\sigma})(\nu,\sigma \in \{x,y\})$ is defined by

$$\mathbf{C} = \beta \begin{pmatrix} \langle \cos q \cos q \rangle_0 & \langle \cos q \sin q \rangle_0 \\ \langle \sin q \cos q \rangle_0 & \langle \sin q \sin q \rangle_0 \end{pmatrix}. \tag{13}$$

Thus, the formal solution is

$$\begin{pmatrix} M_{1,x} \\ M_{1,y} \end{pmatrix} = [\mathbf{I}_2 - \mathbf{C}]^{-1} \mathbf{C} \begin{pmatrix} h_x \\ h_y \end{pmatrix}, \tag{14}$$

where $\mathbf{I}_2$ is the 2×2 unit matrix, and the susceptibility tensor $\boldsymbol{\chi} = (\chi_{\nu\sigma})(\nu,\sigma \in \{x,y\})$ defined by $\vec{M} = \boldsymbol{\chi}\vec{h}$ in the limit $||\vec{h}|| \to 0$ is

$$\boldsymbol{\chi} = [\mathbf{I}_2 - \mathbf{C}]^{-1} \mathbf{C}. \tag{15}$$

Divergence of $\boldsymbol{\chi}$ appears at the critical point satisfying $\det(\mathbf{I}_2 - \mathbf{C}) = 0$.

It is easy to show that the correlation matrix is now expressed by $\mathbf{C} = (\beta/2)\mathbf{I}_2$. The susceptibility tensor is hence diagonalized and the diagonal elements are

$$\chi_{xx} = \chi_{yy} = \frac{\beta/2}{1 - \beta/2} = \frac{T_c}{T - T_c}, \tag{16}$$

with the critical temperature $T_c = 1/2$ of the second-order phase transition [10]. The vanishing off-diagonal elements come from spatial homogeneity of $f_0(p)$, and symmetry of $f_0(p)$ is not necessary.

C. Vlasov linear response

The nonlinear response theory [12] includes the linear response theory [13,14] if $f_0(p)$ depends on p only through

$H_0 = p^2/2$, and provides a simple expression of the linear response [15], but asymmetric $f_0(p)$ is out of range. Thus, we revisit the linear response theory.

We introduce the Laplace transform defined by

$$\widehat{u}(\omega) = \int_0^\infty u(t) e^{i\omega t} \mathrm{d}t. \tag{17}$$

The linear response theory gives the Laplace transform of $(M_{1,x}(t), M_{1,y}(t))$, denoted $(\widehat{M}_{1,x}(\omega), \widehat{M}_{1,y}(\omega))$, as

$$\begin{pmatrix} \widehat{M}_{1,x}(\omega) \\ \widehat{M}_{1,y}(\omega) \end{pmatrix} = [\mathbf{I}_2 - \mathbf{F}(\omega)]^{-1} \mathbf{F}(\omega) \begin{pmatrix} \widehat{h}_x(\omega) \\ \widehat{h}_y(\omega) \end{pmatrix}, \tag{18}$$

where the elements of matrix $\mathbf{F} = (F_{\nu\sigma})$ are

$$\begin{aligned} F_{xx}(\omega) &= \frac{-\pi}{2} \int_L \left(\frac{1}{p-\omega} + \frac{1}{p+\omega} \right) f_0'(p) \mathrm{d}p, \\ F_{xy}(\omega) &= \frac{-\pi}{2i} \int_L \left(\frac{1}{p-\omega} - \frac{1}{p+\omega} \right) f_0'(p) \mathrm{d}p, \\ F_{yx}(\omega) &= -F_{xy}(\omega), \\ F_{yy}(\omega) &= F_{xx}(\omega). \end{aligned} \tag{19}$$

See Appendix A for derivations. The integral contour L is the real p axis for $\mathrm{Im}(\omega) > 0$ but is continuously modified for $\mathrm{Im}(\omega) \leqslant 0$ to avoid the poles at $p = \pm\omega$ by following Landau's procedure [32].

Temporal evolution of $(M_{1,x}, M_{1,y})$ is determined by performing the inverse Laplace transform, which picks up singularities of its Laplace transform, (18). For instance, a pole at ω_L gives a term having $\exp(-i\omega_\mathrm{L} t)$, which implies Landau damping for $\mathrm{Im}(\omega_\mathrm{L}) < 0$. Assuming that the reference $f_0(p)$ is stable, we have no singularities in the upper half-plane of ω. The existence of singularities on the real axis of ω is accidental for $[\mathbf{I}_2 - \mathbf{F}(\omega)]^{-1}\mathbf{F}(\omega)$, and we omit it. Then the main singularity comes from the Heaviside step function of the external field, (6), whose Laplace transform is

$$\begin{pmatrix} \widehat{h}_x(\omega) \\ \widehat{h}_y(\omega) \end{pmatrix} = \frac{-1}{i\omega} \begin{pmatrix} h_x \\ h_y \end{pmatrix}. \tag{20}$$

Asymptotic values of $M_{1,x}$ and $M_{1,y}$ are, therefore, obtained by picking up the pole at $\omega = 0$ [14], and

$$\begin{pmatrix} M_{1,x}(t) \\ M_{1,y}(t) \end{pmatrix} \to \boldsymbol{\chi} \begin{pmatrix} h_x \\ h_y \end{pmatrix} \quad (t \to \infty), \tag{21}$$

where the susceptibility tensor $\boldsymbol{\chi} = (\chi_{\nu\sigma})$ is written in a form similar to (15) as

$$\boldsymbol{\chi} = [\mathbf{I}_2 - \mathbf{F}(0)]^{-1} \mathbf{F}(0). \tag{22}$$

Let us rewrite the above Vlasov susceptibility $\boldsymbol{\chi}$ by using the dispersion function

$$D(\omega) = 1 + \pi \int_L \frac{f_0'(p)}{p-\omega} \mathrm{d}p, \quad \omega \in \mathbb{C}. \tag{23}$$

In the following we consider real ω, which gives

$$D(\omega) = 1 + \pi \mathrm{PV} \int_{-\infty}^{\infty} \frac{f_0'(p)}{p-\omega} \mathrm{d}p + i\pi^2 f_0'(\omega), \quad \omega \in \mathbb{R}, \tag{24}$$

where PV represents the principal value. The dispersion function rewrites the susceptibility as

$$\boldsymbol{\chi} = \frac{1}{|D(0)|^2} \begin{pmatrix} \mathrm{Re(D(0))} - |\mathrm{D(0)}|^2 & -\mathrm{Im}(D(0)) \\ \mathrm{Im}(D(0)) & \mathrm{Re}(D(0)) - |D(0)|^2 \end{pmatrix}. \tag{25}$$

When $f_0(p)$ is symmetric and hence $f_0'(0) = 0$, implying that $\mathrm{Im}(D(0)) = 0$ accordingly, the susceptibility tensor $\boldsymbol{\chi}$ is diagonal, and the diagonal elements are

$$\chi_{xx} = \chi_{yy} = \frac{1 - D(0)}{D(0)} \tag{26}$$

as reported in Refs. [13] and [14]. The susceptibility, therefore, diverges at the point $D(0) = 0$, corresponding to the stability threshold [9,35]. On the other hand, when $f_0'(0) \neq 0$, the imaginary part of $D(0)$ does not vanish and hence the susceptibility tensor, (25), shows two interesting features: (i) The tensor is neither symmetric nor diagonalizable by the real coordinate transformation, since the eigenvalues are not real. (ii) No divergence appears for any $f_0(p)$ including the stability threshold, since $|D(0)|^2 > 0$. We note that, for homogeneous symmetric unimodal distributions, $D(0) > 0$ is the stability criterion and hence the divergence appears at the stability threshold. However, $D(0) > 0$ is no longer the stability criterion for the asymmetric case. A stability criterion for the asymmetric case is introduced in Sec. III B.

III. SKEW-NORMAL DISTRIBUTION AND STABILITY

A. Skew-normal distribution

We introduce the skew-normal distribution for examining the linear response theory and confirming the two features mentioned in Sec. II C. Advantages of the skew-normal distribution are that it has a single peak, which makes the stability criterion simpler, and that the analytically obtained mean value helps to set the total momentum to 0.

The density of skew-normal distribution is defined by

$$f_\mathrm{SN}(x; \lambda, \mu, \sigma) = \frac{2}{\sigma} \phi\left(\frac{x-\mu}{\sigma} \right) \Phi\left(\lambda \frac{x-\mu}{\sigma} \right), \tag{27}$$

where

$$\phi(x) = \frac{1}{\sqrt{2\pi}} e^{-x^2/2} \tag{28}$$

and

$$\Phi(x) = \int_{-\infty}^{x} \phi(t) \mathrm{d}t = \frac{1}{2} \left[1 + \mathrm{erf}\left(\frac{x}{\sqrt{2}} \right) \right]. \tag{29}$$

The parameter λ represents the skewness, and $\lambda = 0$ results in a normal distribution. The mean value is

$$\int_{-\infty}^{\infty} x f_\mathrm{SN} \mathrm{d}x = \mu + \sigma\delta\sqrt{\frac{2}{\pi}}, \quad \delta = \frac{\lambda}{\sqrt{1+\lambda^2}}. \tag{30}$$

We test the homogeneous stationary states of the form

$$f_0(p; \lambda, \mu, \sigma) = \frac{1}{2\pi} f_\mathrm{SN}(p; \lambda, \mu, \sigma), \tag{31}$$

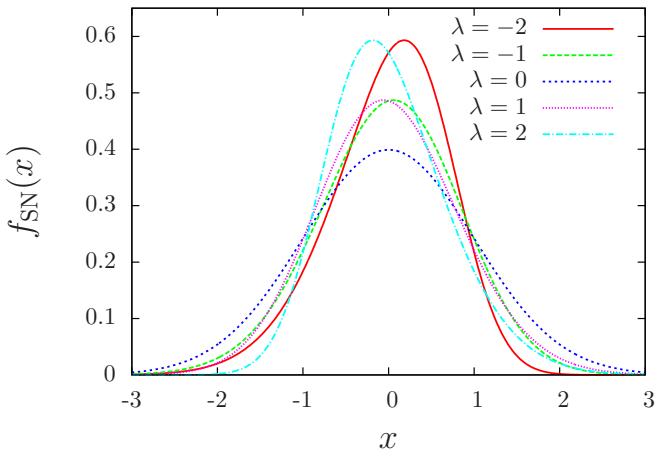

FIG. 1. (Color online) Skew-normal distributions with 0 means and $\sigma = 1$. $\lambda = -2$, -1, 0, 1, and 2; maximum points go from right to left. $f_0'(0)$ is positive (negative) for negative (positive) λ.

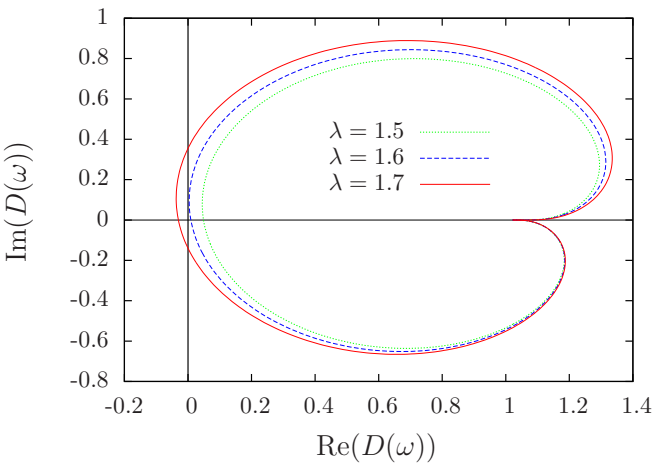

FIG. 2. (Color online) Nyquist diagrams for skew-normal distributions $f_0(p;\lambda)$ with $\lambda = 1.5$ [dotted (green) curve], $\lambda = 1.6$ [dashed (blue) curve], and $\lambda = 1.7$ [solid (red) curve]. Each curve is the mapped real ω axis by D, which intersects with the real $D(\omega)$ axis at $\omega = \eta$, the unique extreme point $p = \eta$ of $f_0(p;\lambda)$. Inside the curve corresponds to the upper half-plane of ω.

which is normalized as $\iint_\mu f_0 \mathrm{d}q\mathrm{d}p = 1$. To set the total momentum to 0, we put

$$\mu = -\sigma\delta\sqrt{\frac{2}{\pi}}. \tag{32}$$

Hereafter we fix the parameter σ at $\sigma = 1$. Then the unique free parameter is the skewness λ, and the distribution is simply denoted $f_0(p;\lambda)$. Let $p = \eta$ be the unique extreme point (the maximum point) depending on λ. Some examples of the skew-normal distribution functions are shown in Fig. 1.

B. Nyquist method of stability

For symmetric unimodal distributions $f_0(p)$, the formal stability criterion has been established [3] as

$$f_0(p) \text{ is formally stable} \iff D(0) > 0, \tag{33}$$

where D is the dispersion function, (24). To obtain the formal stability, $f_0(p)$ is assumed as a function of the one-particle Hamiltonian, and hence we cannot use this criterion for skew-normal distributions. Instead, we use the Nyquist method [33,34], which was applied to asymmetric double-peak distributions in the HMF model [35].

In our setting, the Nyquist method provides the stability criterion as

$$f_0(p;\lambda) \text{ has an exponentially growing mode} \iff D(\eta) < 0, \tag{34}$$

where $D(\omega)$ is the dispersion function, (24), and is real at $\omega = \eta$. See Appendix B for details. The function $D(\eta)$ can be rewritten as

$$D(\eta) = 1 + \pi \int_{-\infty}^{\infty} \frac{f_0(p;\lambda) - f_0(\eta;\lambda)}{(p-\eta)^2}\mathrm{d}p, \tag{35}$$

by performing integration by parts and remembering $f_0'(\eta;\lambda) = 0$ [36]. The Taylor expansion says that the numerator of the integrand starts from the quadratic term, $(p-\eta)^2$, and hence no singularity appears in the integrand. A rigorous treatment of the above Penrose criterion is reported in Ref. [37].

The stability criterion, (34), is graphically presented in Fig. 2. The mapped real ω axis by D intersects with the real $D(\omega)$ axis at $\omega = \eta$ only, since $\mathrm{Im}(D(\omega))$ vanishes at the unique extreme point. Consequently, we can say that the state $f_0(p;\lambda)$ is unstable iff the mapped real ω axis by D crosses with the negative real axis on the complex $D(\omega)$ plane. Figure 2 shows that the stability threshold of the skew-normal distributions, denoted λ_{th}, must be in the interval $1.6 < \lambda_{\mathrm{th}} < 1.7$. From symmetry with respect to λ, we have another threshold, $-\lambda_{\mathrm{th}}$, and $f_0(p;\lambda)$ is stable for $-\lambda_{\mathrm{th}} < \lambda < \lambda_{\mathrm{th}}$.

The stability threshold can be estimated by precise numerical computations. The integral interval in Eq. (35) is infinite, and hence we introduce the cutoff P as

$$D_P(\eta) = 1 + \pi \int_{-P}^{P} \frac{f_0(p;\lambda) - f_0(\eta;\lambda)}{(p-\eta)^2}\mathrm{d}p \tag{36}$$

and observe P dependence of λ_{th}. The estimated threshold with varying P is reported in Fig. 3 and is fitted by $1.622 + 1.463/P$, where the fitting curve is obtained by the least squares method. We hence conclude that the threshold is $\lambda_{\mathrm{th}} \simeq 1.622$ in the limit $P \to \infty$.

IV. NUMERICAL TESTS

We use the semi-Lagrangian code [38] with time slice $\Delta t = 0.05$. The μ space, the (q,p) plane, is truncated to $(-\pi,\pi] \times [-4,4]$ and is divided into $G \times G$ grid points. We call G the grid size. The magnetization is 0 for the reference homogeneous state $f_0(p;\lambda)$, and therefore, we simply denote the response magnetization (M_x, M_y) instead of $(M_{1,x}, M_{1,y})$.

It might be worth remarking that the truncation at $|p| = 4$ does not conflict with the estimation of λ_{th} reported in Fig. 3, which requires a larger cutoff. The reference state f_0 rapidly decreases as the Gaussian, thus the truncation at $|p| = 4$ is reasonable in the semi-Lagrangian code. However, the term $f_0(\eta;\lambda)/(p-\eta)^2$ of the integrand in (36) slowly decreases as

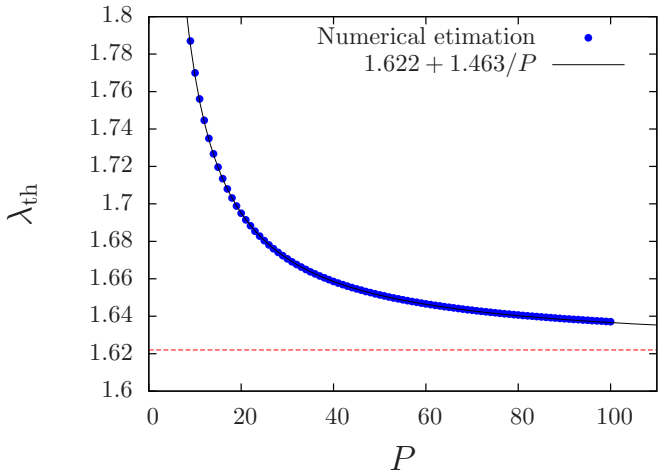

FIG. 3. (Color online) Numerical estimation of threshold $\lambda_{\rm th}$ while varying the cutoff P [filled (blue) circles]. The solid black curve is the fitting by the least squares method in the interval [10,100] of P, and the dashed horizontal (red) line is the estimated level of $\lambda_{\rm th} = 1.622$.

p^{-2} in the large $|p|$, and hence the cutoff P in (36) must be large.

A. Stability threshold and unstable branch

The obtained stability threshold is directly examined by computing the temporal evolution of a perturbed state. We prepare the perturbed initial state as

$$f_\epsilon(q,p;\lambda) = f_0(p;\lambda)(1+\epsilon\cos q) \tag{37}$$

and use $\epsilon = 10^{-6}$. The temporal evolution of $M = (M_x^2 + M_y^2)^{1/2}$ is shown in Fig. 4, and the computed threshold $\lambda_{\rm th}$ is successfully confirmed.

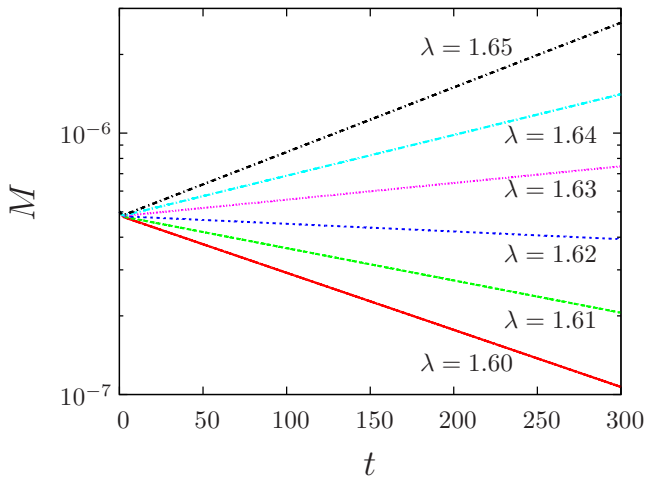

FIG. 4. (Color online) Initial temporal evolutions of M for the perturbed initial state $f_\epsilon(q,p;\lambda)$, (37), with $\epsilon = 10^{-6}$ and $\lambda = 1.60$, 1.61, 1.62, 1.63, 1.64 and 1.65, from bottom to top. The grid size is $G = 512$. The vertical axis is on a logarithmic scale. The stability threshold is in the interval $1.62 < \lambda_{\rm th} < 1.63$, and is consistent with the estimated value $\lambda_{\rm th} \simeq 1.622$.

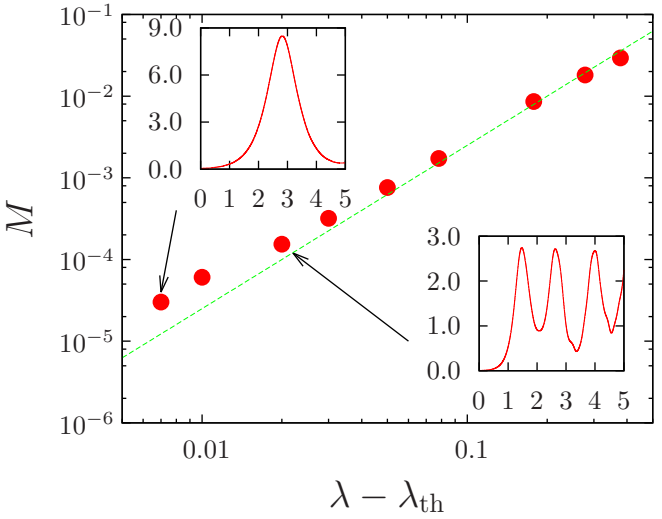

FIG. 5. (Color online) Time-averaged M as a function of $\lambda - \lambda_{\rm th}$ for $f_\epsilon(q,p;\lambda)$, (37), with $\epsilon = 10^{-6}$. The time window for averages is [1000,5000]. The grid size is $G = 512$. The straight diagonal (green) line represents $M = (\lambda - \lambda_{\rm th})^2/4$ and is a guide for the eyes. The insets represent temporal evolutions of M for the marked points. The horizontal axis represents the scaled time $t/1000$, the vertical axes, $10^5 M$ and $10^4 M$ for the upper-left and lower-right insets, respectively.

When the initial state is symmetric with respect to p, the nonlinear response theory [12] predicts that M will be proportional to $(\lambda - \lambda_{\rm th})^2$ in the unstable branch. Numerical simulations captured oscillations of M around the predicted levels and the period tends to increase as the initial state approaches the stability threshold [12]. Even in the present asymmetric case, scaling, oscillations, and a similar tendency of periods are observed as reported in Fig. 5.

B. Linear responses

We come back to the unperturbed initial distribution $f_0(p;\lambda)$ and add the external field (6). From the symmetry of the system we set $(h_x,h_y) = (h,0)$ without loss of generality.

In order to examine the linear response theory, we set $h = 10^{-5}$ to be small enough. The normalized responses M_x/h and M_y/h, which are susceptibilities in the limit $h \to 0$, are reported in Fig. 6 for stable states of $\lambda = 1.2$ and 1.6.

The theoretically predicted levels of responses are in good agreement with the numerical experiments in the initial time intervals. The lifetime of the agreements gets longer as the grid size G increases, and is, roughly speaking, proportional to G. We may therefore conclude that the theoretically predicted response tensor is valid for a long time and that the nonzero off-diagonal response is observable if we use a fine grid.

For the whole stable interval of λ, the theory is compared with numerical results in Fig. 7. We remark that the state with $\lambda = 0$ is the thermal equilibrium state of temperature $T = 1$, and the normalized response M_x/h coincides with the previously computed Vlasov linear response $T_c/(T - T_c) = 1$ [13,14], which also coincides with the isothermal linear response, (16). We stress that, as stated at the end of Sec. II C, no divergence is observed at the stability threshold, which is

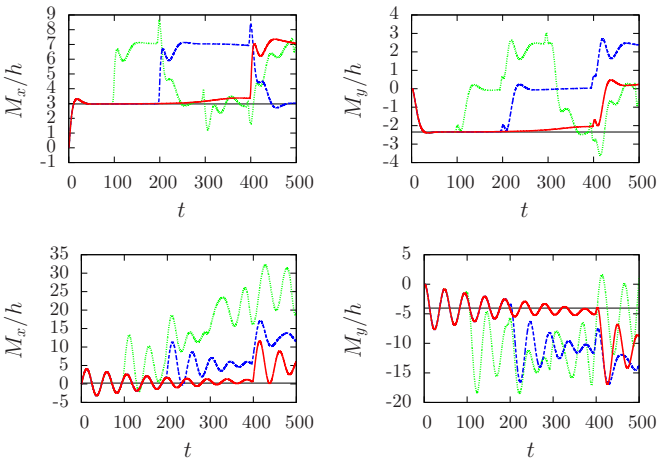

FIG. 6. (Color online) Normalized responses M_x/h (left) and M_y/h (right) with $h = 10^{-5}$. $\lambda = 1.2$ (top) and $\lambda = 1.6$ (bottom). Grid sizes are $G = 128$ [dotted (green) line], $G = 256$ [dashed (blue) line],and $G = 512$ [solid (red) line]. Horizontal black lines are theoretical predictions: $M_x/h = 2.972$ and $M_y/h = -2.344$ for $\lambda = 1.2$, and $M_x/h = 0.2353$ and $M_y/h = -4.042$ for $\lambda = 1.6$.

shown at the left and right boundaries of the figure. Another remark is that the strength of the response $(M_x^2 + M_y^2)^{1/2}/h$ for $\lambda \neq 0$ is higher than in the symmetric case, $\lambda = 0$.

One possible explanation for the sign of χ_{yx} is as follows. We may concentrate for $\lambda > 0$ without loss of generality. In this case the negative part of $f_0(p;\lambda)$ is larger than the positive part around $p = 0$, and hence the small cluster around $p = 0$ induced by the external field locally has a negative total momentum. Consequently, the magnetization vector is turned to the negative direction of q by the external field.

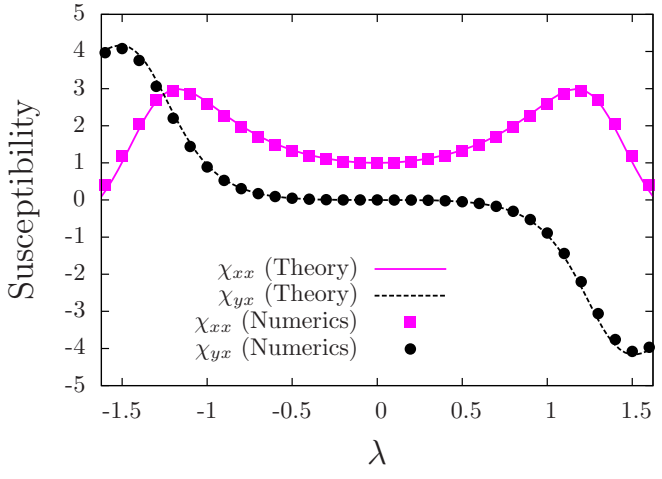

FIG. 7. (Color online) Elements of the susceptibility tensor as a function of the skewness λ. Lines are from theory. Symbols are from numerics with grid size $G = 512$, and M_x and M_y are computed as averages over the time window [0,200]. Diagonal element χ_{xx} [solid (magenta) line with squares] and off-diagonal element χ_{yx} (dashed black line with circles). The interval of λ is restricted in the stable interval.

C. Dependence on the external magnetic field

The present nondiagonalizable susceptibility tensor comes from a nonzero $f_0'(0;\lambda)$, which implies that the maximum point η differs from the origin. Thus, we expect that asymmetric characters of the linear response tend to be hidden if the characteristic scale of the p axis, the width of the separatrix, is larger than the maximum point $p = \eta$, since the local total momentum in the separatrix approaches 0.

For the magnetization (M_x, M_y) and the external field $(h,0)$, the separatrix reaches $|p| = 2\sqrt{||\vec{M}|| + h}$. Magnetization is induced by the external field, and we have

$$||\vec{M}|| = h\sqrt{(\chi_{xx})^2 + (\chi_{yx})^2}. \tag{38}$$

Then we may expect that the asymmetric characters appear for small h, satisfying

$$h < h_{\rm th}, \quad h_{\rm th} = \frac{\eta^2}{4[(\chi_{xx})^2 + (\chi_{yx})^2 + 1]}. \tag{39}$$

We report the h dependence of susceptibilities in Fig. 8 for $\lambda = 1.2$ and 1.6. The normalized responses, M_x/h and M_y/h, approach the theoretically predicted levels in $h < h_{\rm th}$, while the off-diagonal response, M_y/h, goes to 0 for larger h.

V. STATIONARITY AND NONLINEAR EFFECTS

Let us discuss a possible scenario of temporal evolution with an off-diagonal response. First, we show the fact that the predicted state with nonzero M_y is not stationary by stating that $\vec{M}$ and $\vec{h}$ must be parallel in a stationary state.

The Jeans theorem [4,16] states that an inhomogeneous distribution function is a stationary solution of the Vlasov equation if and only if it depends on (q,p) only through integrals of the one-particle Hamiltonian system. The responding state has nonzero (M_x, M_y) and the integral is the Hamiltonian

$$\mathcal{H} = p^2/2 - \tilde{M}\cos(q - \alpha), \tag{40}$$

where

$$\tilde{M} = \sqrt{(M_x + h_x)^2 + (M_y + h_y)^2}, \quad \tan\alpha = \frac{M_y + h_y}{M_x + h_x}. \tag{41}$$

Then, for a stationary state $f(q,p) = F(\mathcal{H}(q,p))$, we have the vanishing integral of

$$0 = \iint_\mu \sin(q - \alpha)F(\mathcal{H}(q,p))\mathrm{d}q\mathrm{d}p = M_y\cos\alpha - M_x\sin\alpha, \tag{42}$$

since the integrand of the middle is odd with respect to $q - \alpha$. This equality and the definition of α imply

$$\frac{M_y + h_y}{M_x + h_x} = \frac{M_y}{M_x}, \tag{43}$$

and we conclude that $\vec{M}$ and $\vec{h}$ are parallel.

As a result, the state predicted by the linear response theory is not a stationary state, and hence the system does not maintain the predicted state as observed in Fig. 6. We point out a similarity of the present phenomenon to nonlinear

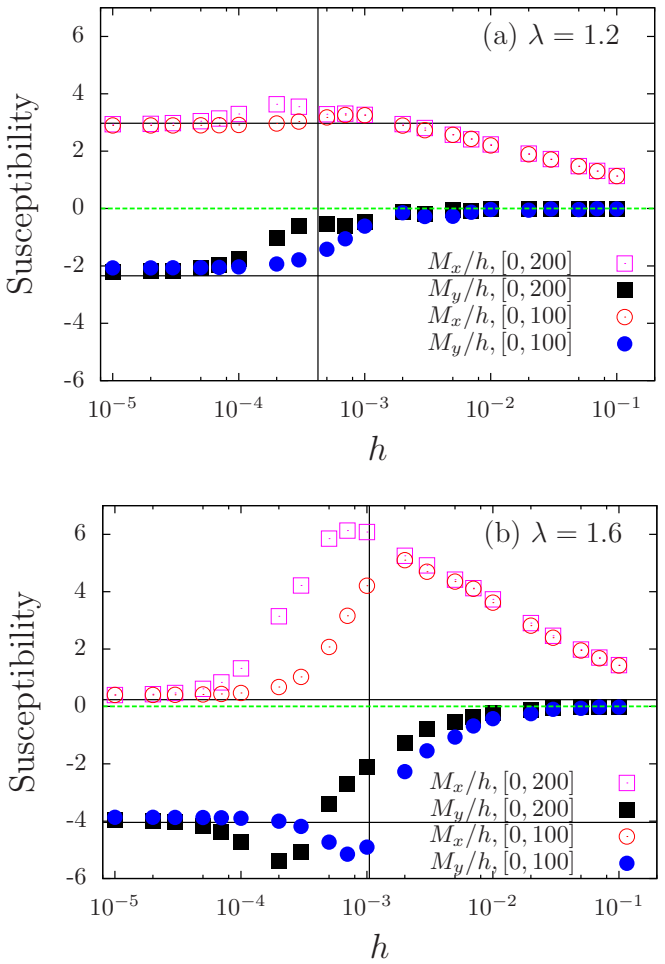

FIG. 8. (Color online) The h dependence of susceptibilities for (a) $\lambda = 1.2$ and (b) $\lambda = 1.6$. Open symbols are for M_x/h, and filled symbols for M_y/h, which are averaged over the time window [0,200] (squares) or [0,100] (circles). Vertical black lines represent $h_{\rm th}$; horizontal black lines, linear response levels. Dashed horizontal (green) lines are the 0 level. The grid size is $G = 512$.

trapping [39]. If the Landau damping time scale is longer than the so-called trapping time scale, then exponential Landau damping stops and a cluster is formed by nonlinear effects [40]. In other words, the state experiences linear Landau damping at an early time interval but the damping stops due to nonlinear effects. Similarly, the state predicted by the linear response theory appears for a short time interval and then disappears. We conjecture that the disappearance is due to the nonlinearity of the full Vlasov equation.

VI. DISCUSSION AND SUMMARY

We have investigated the response tensor against an asymptotically constant external field for spatially homogeneous but asymmetric distributions of momenta with 0 means using the linear response theory. The theory predicts two interesting characters of the susceptibility tensor: One is nondiagonalizablility, and the other is nondivergence even at the stability threshold. The former implies that an external field added in the x direction induces magnetization in the y direction even in the simple HMF model. The off-diagonal response is not mysterious in our setting, since anisotropy is included in the asymmetry of momentum distributions. To realize the theoretical setting, we introduced a family of skew-normal distributions. After studying the stability of the family by the Nyquist method, all the theoretical consequences are successfully confirmed by direct numerical simulations of the Vlasov equation. We stress that the crucial condition for the two characters is a nonzero derivative of the reference state, $f_0'(0) \neq 0$, which never occurs for symmetric $f_0(p)$. One physical example of $f_0'(0) \neq 0$ can be found in a beam-plasma system, whose momentum distribution consists of, for instance, a drifting Maxwellian for the beam and a Maxwellian for the plasma [25]. In this example the nonzero derivative $f_0'(0) \neq 0$ is realized both with and without shifting the distribution to set the total momentum to 0 in general. Studying distributions with two or more peaks is work for the future.

The state reached by the linear response is neither in thermal equilibrium nor in a stationary state, since the off-diagonal response is not 0, while the magnetization and the external field vectors must be parallel in a stationary state. The lifetime of such a state is finite but gets longer as the grid size becomes finer. Thus, we may expect that an off-diagonal response will be experimentally observed with the use of a large enough number of particles. However, nonstationarity may cause shortness of the lifetime compared with the symmetric case, and determining the time scale at which the linear response theory is valid remains for future work.

Related to the above discussion, we remark on the validity of the linear response theory for predicting asymptotic stationary states. We considered stable reference states and added a small enough external field. Nevertheless, asymptotic stationary states cannot be predicted by the linear response theory for asymmetric homogeneous initial states. Comparison with linear Landau damping, which is stopped by nonlinear effects, might be interesting. Recently nonlinear equations for magnetization moments have been proposed for homogeneous water-bag initial distributions in the HMF model under an external field [22]. An extension to non-water-bag states could possibly help us to understand the nonlinear effects and to solve the puzzle of the linear response theory.

In addition to the stable initial states, perturbed unstable asymmetric initial states are also studied, and features similar to those in the symmetric case are numerically observed [12], in ordering and oscillations of magnetization around the saturated states. Apart from the macroscopic variable, an examination of the difference in distribution functions remains to be done. For instance, the core-halo structure [24] has been observed in the μ space for water-bag initial states [21], but it is still unclear whether the present asymmetric unstable states also yield such a structure in saturated states.

In this article we have focused on an asymptotically constant external field corresponding to 0 total momentum, but an oscillating external field of $\cos(\omega_0 t)$ ($\omega_0 \in \mathbb{R}$) is also available. The Laplace transform of the external field provides poles at $\omega = \pm\omega_0$, and the denominator of susceptibility, $|D(0)|^2$, is replaced with $D(\pm\omega_0)\overline{D(\mp\omega_0)}$ as shown in (A15), where $\overline{D(\omega_0)}$ is the complex conjugate of $D(\omega_0)$. As a result, setting $\omega_0 = \eta$, where η is the maximum point of

the momentum distribution, the susceptibility diverges at the stability threshold, which satisfies $D(\eta)=0$. The symmetry is, therefore, not essential for the divergence of susceptibility. Even in this case, the susceptibility tensor has nonzero off-diagonal elements reflecting the asymmetry; see (A19).

ACKNOWLEDGMENTS

The author thanks the anonymous referees for useful comments that improved the manuscript. He acknowledges the support of JSPS KAKENHI Grant No. 23560069.

APPENDIX A: DERIVATION OF THE VLASOV LINEAR RESPONSE

Let X_0 be the Hamiltonian vector field associated with the Hamiltonian H_0, (7), which is expressed as

$$X_0 = p\frac{\partial}{\partial q}. \tag{A1}$$

Linearizing the Vlasov equation, (4), around $f_0(p)$, we have the formal solution of perturbation $f_1(q,p,t)$ as

$$f_1(q,p,t) = -\int_0^t e^{-(t-s)X_0}\{H_1(s), f_0\}\mathrm{d}s \tag{A2}$$

for the initial condition $f_1(q,p,t=0)=0$. The operator $\exp(tX_0)$ acts on a function $u(q,p)$ as

$$e^{tX_0}u(q,p) = u(\varphi_0^t(q,p)), \tag{A3}$$

where φ_0^t is the Hamiltonian flow associated with H_0 and hence $\varphi_0^t(q,p)=(q+pt,t)$ in our setting. We can prove the equality

$$\iint_\mu v(q,p)u(\varphi_0^{-t}(q,p))\mathrm{d}q\mathrm{d}p = \iint_\mu v(\varphi_0^t(q,p))u(q,p)\mathrm{d}q\mathrm{d}p \tag{A4}$$

by changing variables $(q',p')=\varphi_0^{-t}(q,p)$ and using $\mathrm{d}q'\mathrm{d}p' = \mathrm{d}q\mathrm{d}p$ from the canonical property of φ_0^t. Thus, we have

$$\langle B\rangle_1(t) = -\iint_\mu \mathrm{d}q\mathrm{d}p\int_0^t B_{t-s}(q,p)\{H_1(s), f_0\}\mathrm{d}s, \tag{A5}$$

where $B_t(q,p)=B(\varphi_0^t(q,p))$. Performing the Laplace transform, (17), we obtain

$$\widehat{\langle B\rangle}_1(\omega) = -\iint_\mu \widehat{B}_\omega(q,p)\{\widehat{H}_1(q,\omega), f_0(p)\}\mathrm{d}q\mathrm{d}p, \tag{A6}$$

with

$$\begin{aligned}\widehat{H}_1(q,\omega) = &-[\widehat{M}_{1,x}(\omega)+\widehat{h}_x(\omega)]\cos q\\ &-[\widehat{M}_{1,y}(\omega)+\widehat{h}_y(\omega)]\sin q.\end{aligned} \tag{A7}$$

Substituting $B=\cos q$ and $B=\sin q$ into the linear response formula, (A6), and using the Laplace transforms of $\cos q_t=\cos(q+pt)$ and $\sin q_t=\sin(q+pt)$, which are, respectively,

$$\widehat{\cos q}_\omega = \frac{1}{2i}\left(\frac{e^{-iq}}{p-\omega}-\frac{e^{iq}}{p+\omega}\right) \tag{A8}$$

and

$$\widehat{\sin q}_\omega = \frac{1}{2}\left(\frac{e^{-iq}}{p-\omega}+\frac{e^{iq}}{p+\omega}\right), \tag{A9}$$

we have the matrix form of

$$\begin{pmatrix}\widehat{M}_{1,x}(\omega)\\ \widehat{M}_{1,y}(\omega)\end{pmatrix} = \begin{pmatrix}F_{xx}(\omega) & F_{xy}(\omega)\\ F_{yx}(\omega) & F_{yy}(\omega)\end{pmatrix}\left[\begin{pmatrix}\widehat{M}_{1,x}(\omega)\\ \widehat{M}_{1,y}(\omega)\end{pmatrix}+\begin{pmatrix}\widehat{h}_x(\omega)\\ \widehat{h}_y(\omega)\end{pmatrix}\right]. \tag{A10}$$

The elements of matrix $\mathbf{F}$ are exhibited in (19).

To ensure convergence of the Laplace transform, (17), matrix $\mathbf{F}(\omega)$ is defined in the upper half-plane of ω. We analytically continue the domain into the whole complex ω plane [32], and the integral with the contour L is continued as

$$\int_L \frac{f_0'(p)}{p\mp\omega}\mathrm{d}p = \mathrm{PV}\int_{-\infty}^{\infty}\frac{f_0'(p)}{p\mp\omega}\mathrm{d}p \pm S(\omega)i\pi f_0'(\pm\omega), \tag{A11}$$

where PV represents the principal value and is the normal integral for $\omega\notin\mathbb{R}$, and the second term, including

$$S(\omega) = \begin{cases}0, & \mathrm{Im}(\omega)>0,\\ 1, & \mathrm{Im}(\omega)=0,\\ 2, & \mathrm{Im}(\omega)<0,\end{cases} \tag{A12}$$

comes from the residues.

We remark that the linear response, (A6), is rewritten as

$$\widehat{\langle B\rangle}_1(\omega) = -\langle\{\widehat{B}_\omega(q,p), \widehat{H}_1(q,\omega)\}\rangle_0, \tag{A13}$$

if we perform integration by parts. Expression (A13) gives a similar form of matrix $\mathbf{F}$ with correlation matrix $\mathbf{C}$, (13), as

$$\mathbf{F}(\omega) = \begin{pmatrix}\langle\{\widehat{\cos q}_\omega, \cos q\}\rangle_0 & \langle\{\widehat{\cos q}_\omega, \sin q\}\rangle_0\\ \langle\{\widehat{\sin q}_\omega, \cos q\}\rangle_0 & \langle\{\widehat{\sin q}_\omega, \sin q\}\rangle_0\end{pmatrix}. \tag{A14}$$

Matrix $\mathbf{F}$ coincides with correlation matrix $\mathbf{C}$ as $\mathbf{F}(\omega)=(\beta/2)\mathbf{I}_2$ if $f_0(p)$ is the Maxwellian with the inverse temperature β. Therefore, the Vlasov linear response coincides with the isothermal linear response at thermal equilibrium of the homogeneous phase [13,14].

In the text we concentrate on the response to the external field with $\omega=0$, but a general ω is also available. The explicit form of the matrix $[\mathbf{I}_2-\mathbf{F}(\omega)]^{-1}\mathbf{F}(\omega)$ is

$$[\mathbf{I}_2-\mathbf{F}(\omega)]^{-1}\mathbf{F}(\omega) = \frac{1}{D(\omega)\overline{D(-\overline{\omega})}}\begin{pmatrix}G(\omega) & F_{xy}(\omega)\\ -F_{xy}(\omega) & G(\omega)\end{pmatrix}, \tag{A15}$$

where $\overline{\omega}$ is the complex conjugate of ω and

$$G(\omega) = [1-F_{xx}(\omega)]F_{xx}(\omega) - [F_{xy}(\omega)]^2. \tag{A16}$$

In particular, the off-diagonal element is written as

$$\begin{aligned}F_{xy}(\omega) = &-\frac{\pi}{2i}\left[\mathrm{PV}\int_{-\infty}^{\infty}\frac{f_0'(p)}{p-\omega}\mathrm{d}p - \mathrm{PV}\int_{-\infty}^{\infty}\frac{f_0'(p)}{p+\omega}\mathrm{d}p\right]\\ &-S(\omega)\frac{\pi^2}{2}[f_0'(\omega)+f_0'(-\omega)]\end{aligned} \tag{A17}$$

and results in $-\mathrm{Im}(D(0)) = -\pi^2 f_0'(0)$ at $\omega=0$ as shown by the susceptibility, (25). If we consider the oscillating external field of $\cos(\omega_0 t)$ ($\omega_0\in\mathbb{R}$), the susceptibility becomes

$$2\boldsymbol{\chi} = [\mathbf{I}_2-\mathbf{F}(\omega_0)]^{-1}\mathbf{F}(\omega_0) + [\mathbf{I}_2-\mathbf{F}(-\omega_0)]^{-1}\mathbf{F}(-\omega_0). \tag{A18}$$

Thus, for $\omega_0 = \eta$, where η is the unique extreme point of $f_0(p)$, the diagonal elements of susceptibility diverge at the stability threshold satisfying $D(\eta) = 0$. Even in this case, the oscillating external field gives the nonzero off-diagonal element as

$$\chi_{xy} = \frac{-\pi^2 f_0'(-\eta)/2}{\left(1 + \pi \mathrm{PV} \int \frac{f_0'(p)}{p+\eta} \mathrm{d}p\right)^2 + (\pi^2 f_0'(-\eta))^2}. \quad \text{(A19)}$$

APPENDIX B: THE NYQUIST METHOD

To review the Nyquist method, we restrict ourselves to single-peak distributions including skew-normal distributions. Let us define the set $R = \{D(\omega) \in \mathbb{C} | \mathrm{Im}(\omega) > 0\}$, where $D(\omega)$ is the dispersion function, (23). If this set R includes the origin, then there exists a root of the dispersion relation $D(\omega)$ in the upper half-plane of ω, and the root corresponds to an exponential growing mode from the definition of the Laplace transform, (17).

To study set R, we investigate the boundary

$$\partial R = \{D(\omega) \in \mathbb{C} | \mathrm{Im}(\omega) = 0\}.$$

The boundary forms a closed curve, since $D(\omega) \to 1$ as $\omega \to \pm\infty$. In the limits of $\omega \to -\infty$ and $+\infty$, the curve approaches 1 from the positive and the negative imaginary sides, respectively, since $f_0'(p) > 0$ for $p < \eta$ and $f_0'(p) < 0$ for $p > \eta$, where η is the maximum point of the single-peak distribution $f_0(p)$. Then the orientation implies that the upper half-plane of ω is mapped inside of the closed curve. The imaginary part of $D(\omega)$ is proportional to $f_0'(\omega)$ for ω real and vanishes if and only if ω coincides with the unique extreme point η. Thus, $D(\eta)$ is real and $D(\eta) < 0$ implies that there is a root of $D(\omega)$ on the upper half-plane (see Fig. 2).

[1] A. Campa, T. Dauxois, and S. Ruffo, Statistical mechanics and dynamics of solvable models with long-range interactions, Phys. Rep. **480**, 57 (2009).

[2] D. H. Zanette and M. A. Montemurro, Dynamics and nonequilibrium states in the Hamiltonian mean-field model: A closer look, Phys. Rev. E **67**, 031105 (2003).

[3] Y. Y. Yamaguchi, J. Barré, F. Bouchet, T. Dauxois, and S. Ruffo, Stability criteria of the Vlasov equation and quasi-stationary states of the HMF model, Physica A **337**, 36 (2004).

[4] J. Binney and S. Tremaine, *Galactic Dynamics (Second Edition)* (Princeton University Press, Princeton, NJ, 2008).

[5] W. Braun and K. Hepp, The Vlasov dynamics and its fluctuations in the $1/N$ limit of interacting classical particles, Commun. Math. Phys. **56**, 101 (1977).

[6] R. L. Dobrushin, Vlasov equations, Funct. Anal. Appl. **13**, 115 (1979).

[7] H. Spohn, *Large Scale Dynamics of Interacting Particles* (Springer-Verlag, Heidelberg, 1991).

[8] J. Barré, F. Bouchet, T. Dauxois, S. Ruffo, and Y. Y. Yamaguchi, The Vlasov equation and the Hamiltonian mean-field model, Physica A **365**, 177 (2006).

[9] S. Inagaki and T. Konishi, Dynamical stability of a simple model similar to self-gravitating systems, Publ. Astron. Soc. Japan **45**, 733 (1993).

[10] M. Antoni and S. Ruffo, Clustering and relaxation in Hamiltonian long-range dynamics, Phys. Rev. E **52**, 2361 (1995).

[11] S. Ogawa, A. Patelli, and Y. Y. Yamaguchi, Non-mean-field critical exponent in a mean-field model: Dynamics versus statistical mechanics, Phys. Rev. E **89**, 032131 (2014).

[12] S. Ogawa and Y. Y. Yamaguchi, Nonlinear response for external field and perturbation in the Vlasov system, Phys. Rev. E **89**, 052114 (2014).

[13] A. Patelli, S. Gupta, C. Nardini, and S. Ruffo, Linear response theory for long-range interacting systems in quasistationary states, Phys. Rev. E **85**, 021133 (2012).

[14] S. Ogawa and Y. Y. Yamaguchi, Linear response theory in the Vlasov equation for homogeneous and for inhomogeneous quasistationary states, Phys. Rev. E **85**, 061115 (2012).

[15] S. Ogawa and Y. Y. Yamaguchi, Landau-like theory for universality of critical exponents in quasistationary states of isolated mean-field systems, Phys. Rev. E **91**, 062108 (2015).

[16] J. H. Jeans, On the theory of star-streaming and the structure of the universe, Mon. Not. R. Astron. Soc. **76**, 70 (1915).

[17] A. Antoniazzi, D. Fanelli, J. Barré, P. H. Chavanis, T. Dauxois, and S. Ruffo, Maximum entropy principle explains quasistationary states in systems with long-range interactions: The example of the Hamiltonian mean-field model, Phys. Rev. E **75**, 011112 (2007).

[18] P. H. Chavanis, Lynden-Bell and Tsallis distributions for the HMF model, Eur. Phys. J. B **53**, 487 (2006).

[19] A. Antoniazzi, F. Califano, D. Fanelli, and S. Ruffo, Exploring the Thermodynamic Limit of Hamiltonian Models: Convergence to the Vlasov Equation, Phys. Rev. Lett. **98**, 150602 (2007).

[20] A. Antoniazzi, D. Fanelli, S. Ruffo, and Y. Y. Yamaguchi, Nonequilibrium Tricritical Point in a System with Long-Range Interactions, Phys. Rev. Lett. **99**, 040601 (2007).

[21] R. Pakter and Y. Levin, Core-Halo Distribution in the Hamiltonian Mean-Field Model, Phys. Rev. Lett. **106**, 200603 (2011).

[22] R. Pakter and Y. Levin, Non-equilibrium dynamics of an infinite range *XY* model in an external field, J. Stat. Phys. **150**, 531 (2013).

[23] Y. Y. Yamaguchi, F. Bouchet, and T. Dauxois, Algebraic correlation functions and anomalous diffusion in the Hamiltonian mean field model, J. Stat. Mech. (2007) P01020.

[24] Y. Levin, R. Pakter, F. B. Rizzato, T. N. Teles, and F. P. C. Benetti, Nonequilibrium statistical mechanics of systems with long-range interactions, Phys. Rep. **535**, 1 (2014).

[25] J. D. Crawford, Amplitude equations on unstable manifolds: singular behavior from neutral modes, in *Modern Mathematical Methods in Transport Theory* (Operator Theory: Advances and Applications, Vol. 51), W. Greenberg and J. Polewczak (eds.) (Birkhäuser Verlag, Basel, 1991), pp. 97–108.

[26] J. D. Crawford, Amplitude equations for electrostatic waves: Universal singular behavior in the limit of weak instability, Phys. Plasmas **2**, 97 (1995).

[27] B. T. Tsurutani and G. S. Lakhina, Some basic concepts of wave-particle interactions in collisionless plasmas, Rev. Geophys. **35**, 491 (1997).

[28] M. Karlický and J. Kašparová, Electron beam – plasma system with the return current and directivity of its X-ray emission, Astronomy & Astrophysics **506**, 1437 (2009).

[29] J. Castro, G. Bannasch, P. McQuillen, T. Pohl, and T. C. Killian, Creating non-Maxwellian velocity distributions in ultracold plasmas, AIP Conf. Proc. **1421**, 31 (2012).
[30] J. Barré, T. Dauxois, G. De Ninno, D. Fanelli, and S. Ruffo, Statistical theory of high-gain free-electron laser saturation, Phys. Rev. E **69**, 045501(R) (2004).
[31] S. Gupta and D. Mukamel, Quasistationarity in a model of classical spins with long-range interactions, J. Stat. Mech. (2011) P03015.
[32] L. Landau, On the vibrations of the electronic plasma, J. Phys. USSR **10**, 25 (1946).
[33] H. Nyquist, Regeneration theory, Bell System Tech. J. **11**, 126 (1932).
[34] D. R. Nicholson, *Introduction to Plasma Theory* (Krieger Publishing Company, Florida, 1992).
[35] P. H. Chavanis and L. Delfini, Dynamical stability of systems with long-range interactions: application of the Nyquist method to the HMF model, Eur. Phys. J. B **69**, 389 (2009).
[36] O. Penrose, Electrostatic instabilities of a uniform non-Maxwellian plasma, Phys. Fluids **3**, 258 (1960).
[37] E. Faou and F. Rousset, Landau damping in Sobolev spaces for the Vlasov-HMF model, arXiv:1403.1668.
[38] P. de Buyl, Numerical resolution of the Vlasov equation for the Hamiltonian mean-field model, Commun. Nonlinear Sci. Numer. Simulat. **15**, 2133 (2010).
[39] T. O'Neil, Collisionless damping of nonlinear plasma oscillations, Phys. Fluids **8**, 2255 (1965).
[40] J. Barré and Y. Y. Yamaguchi, Small traveling clusters in attractive and repulsive Hamiltonian mean-field models, Phys. Rev. E **79**, 036208 (2009).